Article

Comparison of Properties of the Hybrid and Bilayer MWCNTs—Hydroxyapatite Coatings on Ti Alloy

Beata Majkowska-Marzec [1], **Dorota Rogala-Wielgus** [1], **Michał Bartmański** [1], **Bartosz Bartosewicz** [2] **and Andrzej Zieliński** [1,*]

[1] Department of Materials Engineering and Bonding, Gdansk University of Technology, Narutowicza 11/12 str., 80-233 Gdansk, Poland; beamajko@pg.edu.pl (B.M.-M.); dorota.wielgus@pg.edu.pl (D.R.-W.); michal.bartmanski@pg.edu.pl (M.B.)

[2] Institute of Optoelectronics, Military University of Technology, gen. Sylwestra Kaliskiego 2 str., 00-908 Warsaw, Poland; bartosz.bartosewicz@wat.edu.pl

[*] Correspondence: andrzej.zielinski@pg.edu.pl; Tel.: +48-501-329-368; Fax: +48-583471815

Abstract: Carbon nanotubes are proposed for reinforcement of the hydroxyapatite coatings to improve their adhesion, resistance to mechanical loads, biocompatibility, bioactivity, corrosion resistance, and antibacterial protection. So far, research has shown that all these properties are highly susceptible to the composition and microstructure of coatings. The present research is aimed at studies of multi-wall carbon nanotubes in three different combinations: multi-wall carbon nanotubes layer, bilayer coating composed of multi-wall carbon nanotubes deposited on nanohydroxyapatite deposit, and hybrid coating comprised of simultaneously deposited nanohydroxyapatite, multi-wall carbon nanotubes, nanosilver, and nanocopper. The electrophoretic deposition method was applied for the fabrication of the coatings. Atomic force microscopy, scanning electron microscopy and X-ray electron diffraction spectroscopy, and measurements of water contact angle were applied to study the chemical and phase composition, roughness, adhesion strength and wettability of the coatings. The results show that the pure multi-wall carbon nanotubes layer possesses the best adhesion strength, mechanical properties, and biocompatibility. Such behavior may be attributed to the applied deposition method, resulting in the high hardness of the coating and high adhesion of carbon nanotubes to the substrate. On the other hand, bilayer coating, and hybrid coating demonstrated insufficient properties, which could be the reason for the presence of soft porous hydroxyapatite and some agglomerates of nanometals in prepared coatings.

Keywords: hardness; adhesion; hydroxyapatite; carbon nanotubes; titanium; biomedical applications

1. Introduction

Carbon nanotube coatings (CNTs) demonstrate unique mechanical and biological properties. Thanks to this, they are increasingly applied in medicine and diagnostics, including tissue engineering [1,2]. These two-dimensional carbon structures are used, among others, to functionalize materials designed for implants, where CNTs can support osseointegration [3,4].

The biocompatibility of CNTs in orthopedic applications was established by in vitro studies, which showed accelerated bone growth and increased proliferation and differentiation of osteoblasts [5–10]. The most popular kind of metal substrate for CNTs is titanium [3,11–18], which combines some beneficial mechanical properties and biocompatibility with a chemical in vivo susceptibility [11]. Several studies evaluated the body's reaction in the presence of carbon nanotubes, demonstrating a high vitality of osteoblasts compared to the pure titanium substrate [14–16,19]. The

ceramic coating consisting of multiple functionalized CNTs with carboxyl groups and hydroxyapatite (HAp) was reported to enhance mechanical properties and biological adhesion, as well as the response of osteoblasts [20–23]. CNTs have a unique chemical structure, so it could serve as a carrier, e.g., of an antibiotic [11] or other substances [21], able to prevent or cure potential infection in place of implantation and protect against implant rejection.

Nevertheless, possible toxicity of nanomaterials limits CNTs' medical applications [24], even though reports to date are scarce and inconclusive, e.g., for the neurotoxic effects of CNTs [25], or CNTs formation of reactive oxygen species [26]. There are more reports on the lack of adverse effects of CNTs than on their long-term toxicity [24]. Recent toxicological studies performed with the liver and kidney cells showed no adverse outcome [23]. In another study, neither SWCNTs (Single-Wall CNTs) nor MWCNTs (Mulit-Wall CNTs) demonstrated in vitro cytotoxicity for fibroblasts and hippocampal cells [27]. Moreover, CNTs are extensively investigated as components of biocoatings [2], e.g., for the Mg-phosphate coating reinforced by SiC nanowire-CNTs [28], HAp-CNTs composite coating on Mg alloy [29], SWCNTs/HAp and MWCNTs on Ti and its alloys [14–17]. Thus, the cytotoxicity of CNTs is generally assumed to be negligible. Even the use of both SWCNTs and MWCNTs as a base liquid with human blood was reported [30].

Pure SWCNTs, as well as MWCNTs coatings, have been obtained [31–33], but the composite or hybrid layers are even more extensively developed as, e.g., CNTs–HAp [13,22,23,34–37] or CNTs–graphene oxide [38]. Most frequently, the electrophoretic deposition (EPD) [12,14,39–41], electrocathodic deposition [15,16,20] or chemical vapor deposition (CVD) processes [42] are applied to prepare CNTs coating.

In the case of materials intended for dental or orthopedic load-bearing implants, adhesion and bond strength are essential, especially at the stage of implantation and ingrowth of human tissue. As Gopi et al. observed, the addition of low amounts of MWCNTs (0.5 and 1 mass pct.) increases hardness, and Young's modulus of the sol-gel derived HAp/MWCNTs coatings [15]. Nevertheless, the concentration of 1% and 2% of CNTs in the composite did not affect adhesion strength significantly and reached 24.2 and 22.4 MPa, respectively [16]. Mukherjee et al. reported an improvement of fracture toughness, flexural and impact strength values for MWCNTs-reinforced HAp [23]. The interfacial shear strength and the maximum load-bearing capacity of the tested CNTs–Ti interfaces were assessed at 37.8 MPa and 245 nN, respectively [43]. The tape tests displayed high adhesion strength (class 5B) for CNTs–(Zn)HAp coating [18]. In another work, the addition of CNTs to the Ti–HAp composite improved both the adhesion strength and hardness for the Ni–Ti substrate [35]. The highest bonding strength of 25.7 MPa was reported for the SWNTs/HAp coating and was nearly 70% more elevated than that of the pure HAp coating [17]. Better mechanical properties were observed for new complex hybrid materials, such as MWCNTs-HAp [20] and fluorohydroxyapatite (FA)-CNTs coating deposited on the TiO_2 nanotubular layer [44]. In the last case, CNTs served as a reinforcement, because of their higher elastic modulus compared to the FA matrix. The homogeneous distribution of decorated CNTs resulted in the robust interface between FA and CNTs. CNT-reinforced HAp composites had substantially better bending strength and fracture toughness than pure HAp [45]. Thus, the presence of MWCNTs evidently improves cohesion, but its adhesion to titanium substrate is less known and may be dependent on the specific architecture of a coating.

In sum, all the investigated material features such as biocompatibility, adhesion strength, and corrosion resistance are highly sensitive to coating composition and microstructure. The objective of the present research is to assess the adhesion strength, mechanical properties of coatings and wettability for the pure MWCNTs layer, hybrid CNTs–nanohydroxyapatite (nanoHAp) coating, and composite coating. Three different methods of deposition of carbon nanotubes were applied to obtain such coatings: (i) deposition of MWCNTs on a substrate surface, (ii) deposition of nanoHAp coating followed by the deposition of MWCNTs, and (iii) joint deposition of a mixture of nanoHAp, MWCNTs, and some nanometals. The purpose of such a choice lies in the fundamental importance of adhesion for the application of such surface treatment of load-bearing implants, because of the high stresses imposed on them during implantation surgery and the post-implantation period.

2. Materials and Methods

2.1. Preparation of Substrate Surfaces

The Ti13Nb13Zr alloy of the composition shown in Table 1 was used as a substrate. Specimens with a 40 mm diameter were cut from the rods. The surface was ground using abrasive paper SiC up to grit # 800. Then, the samples were rinsed with acetone, distilled water, air-dried, pickled in 5% HF for 30 s to remove oxide layers from the surface and finally rinsed with distilled water.

Table 1. Chemical composition of the Ti13Nb13Zr alloy.

Element	Nb	Zr	Fe	C	H	O	S	Hf	Ti
wt. pct.	13.18	13.49	0.085	0.035	0.004	0.078	<0.001	0.055	rem.

2.2. Preparation of CNTs' Suspension

To prepare the coatings, MWCNTs (3D-nano, number of walls 3–15, outer diameter 5–20 nm, inner diameter 2–6 nm, and length 1–10 μm) were functionalized in a mixture of concentrated sulfuric and nitric acid to add carboxyl groups and to provide a negative charge on the surface of carbon nanotubes. Four hundred and eighty grams of powder was annealed in a vacuum furnace (PROTHERM PC442, Ankara, Turkey) for 8 h at 400 °C and then dispersed in deionized water in an ultrasonic homogenizer (Bandelin Sonopuls HD 2070, Berlin, Germany). The suspension was added to 200 mL of mixed H_2SO_4 and at a ratio of 3:1 *v/v* and heated at 70 °C for 2 h [3]. To prepare the suspension of carbon nanotubes, the reaction mixture was centrifuged and washed several times with water or isopropanol until a neutral pH was reached. The concentration of CNTs in the obtained suspension was 0.27 wt.% in water and 0.4 wt.% in isopropanol. Final suspensions were sonicated for 1 min using an ultrasonic homogenizer to disperse the CNTs well after centrifugation. To prepare the mixed coating (m0.4CNT), 1.25 mL of 0.4 wt.% suspension of carbon nanotubes in isopropanol and 0.1 g of nanohydroxyapatite (grain size distribution approximately 20 nm, 99.8% purity, MKnano, Missisauga, Canada) were dispersed in 100 mL of ethyl alcohol (99.8% purity, Sigma Aldrich, St. Louis, MI, USA) and then mixed with 0.005 g of nanosilver (grain size distribution approx. 30 nm, Hongwu International Group Ltd., Guangzhou, China) and 0.005 g of nanocopper (grain size distribution approximately 80 nm, Hongwu International Group Ltd.) before carrying out the electrophoretic deposition (EPD) process.

2.3. Deposition of Coatings

The electrophoretic deposition (EPD) method was used to prepare the coatings. Their synthesis parameters are shown in Table 2. The Ti13Nb13Zr substrate was used as an anode and platinum as a counter electrode. The electrodes were placed parallel to each other at a distance of 5 mm and connected to a DC power source (MCP/SPN110-01C, Shanghai MCP Corp., Shanghai, China). The coatings were heated in a tubular furnace (PROTHERM PC442) from room temperature to 800 °C at a rate of 200 °C/h and cooled to room temperature with the oven.

Table 2. Parameters of synthesis of the coatings with multi-walled carbon nanotubes.

Coating	Synthesis Stage	Concentration of MWCNTs [%]	Duration of EPD [min]	EDP Voltage [V]	Temperature [°C]
0.27CNT	EPD of MWCNTs	0.27	2	11	ambient
H0.27CNT	EPD of nanoHAp	–	2	30	ambient
	Sintering	–	120	–	800
	EPD of MWCNTs	0.27	2	30	ambient
m0.4CNT	EPD of MWCNTs, nanoHAp, nanosilver, nanocopper	0.4	2	30	ambient
	Sintering	–	120	–	800

2.4. Structure and Morphology

An atomic force microscope (AFM NaniteAFM, Nanosurf, Bracknell, Great Britain) was used to study the surface topography. The examinations were performed in the non-contact mode at 20 mN force. The average roughness index S_a values were estimated based on 512 lines made in the area of 80.4×80.4 μm^2.

The specimens' surfaces were observed using a high-resolution scanning electron microscope (SEM JEOL JSM-7800F, Tokyo, Japan) with a LED detector, at a 5 kV acceleration voltage.

The chemical composition of the coatings was investigated by an X-ray energy dispersive spectrometer (EDS Edax Inc., Mahwah, NJ, USA).

2.5. Nanomechanical Studies

Nanoindentation tests were performed with the NanoTest™ Vantage (Micro Materials, Wrexham, Great Britain) using a Berkovich three-sided pyramidal diamond. Twenty-five (5 × 5) measurements were carried out on each sample. The maximum applied force was 10 mN, the loading and unloading times were set up at 20 s and the dwell period at maximum load was 10 s. The distance between the subsequent indents was 20 μm. During the indent, the load–displacement curve was determined using the Oliver and Pharr method. Based on the load–penetration depth curves, the surface hardness (H) and Young's modulus (E) were calculated using integrated software. Estimating Young's modulus (E), the Poisson's ratio of 0.25 was assumed for carbon nanotube coatings and 0.36 for Ti13Nb13Zr.

Nanoscratch tests were performed with NanoTest™ Vantage (Micro Materials) using a Berkovich three-sided pyramidal diamond. The scratch tests were made by increasing the load from 0 to 200 mN at a loading rate of 1.3 mN/s at a distance of 500 μm. The adhesion of the coating was assessed based on the observation of an abrupt change in frictional force during the test.

2.6. Contact Angle Studies

Water contact angle measurements were carried out by falling drop method using a contact angle instrument (Contact Angle Goniometer, Zeiss, Oberkochen, Germany) at room temperature 10 s after drop out.

3. Results and Discussion

3.1. Structure and Morphology

Figure 1A,B show the AFM images of the topography of the native material, where substantial roughness of the surface after grinding and etching may be observed. After etching, the native material shows higher surface roughness.

Figure 1C–E illustrate the surface topography of the examined coatings composed of, respectively, carbon nanotubes (0.27CNT), carbon nanotubes deposited on the nanohydroxyapatite layer (H0.27CNT) and the composite of carbon nanotubes, nanohydroxyapatite, nanosilver and nanocopper (m0.4CNT). The addition of nanoHAp significantly increases roughness. Such a result may mean that the HAp penetrates through free spaces among nanotubes only a small amount. Fathyunes et al. (2018) proposed that during electrodeposition the water reduction produces hydroxyl ions, causing an increase in the pH near the cathode. Then, the CaP ceramics become insoluble and precipitate on the surface of the titanium substrate [46].

Figure 2 presents the SEM images of the surface topography of carbon nanotubes (0.27CNT), hybrid coating (H0.27CNT), and composite coating (m0.4CNT) together with their EDS spectra, confirming the formation of individual coatings. The carbon nanotubes can be distinguished for each specimen.
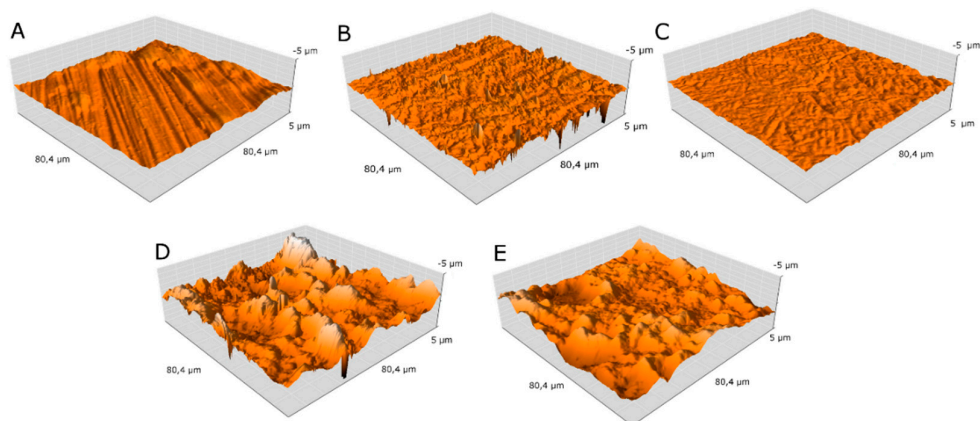
Figure 1. Atomic force microscope (AFM) surface topography of the: (**A**) reference sample—native material after grinding (MR), (**B**) reference sample—after etching (MRe), (**C**) sample of carbon nanotubes (0.27CNT), (**D**) sample of carbon nanotubes deposited on the nanohydroxyapatite layer(H0.27CNT), (**E**) sample of composite of carbon nanotubes, nanohydroxyapatite, nanosilver and nanocopper (m0.4CNT).
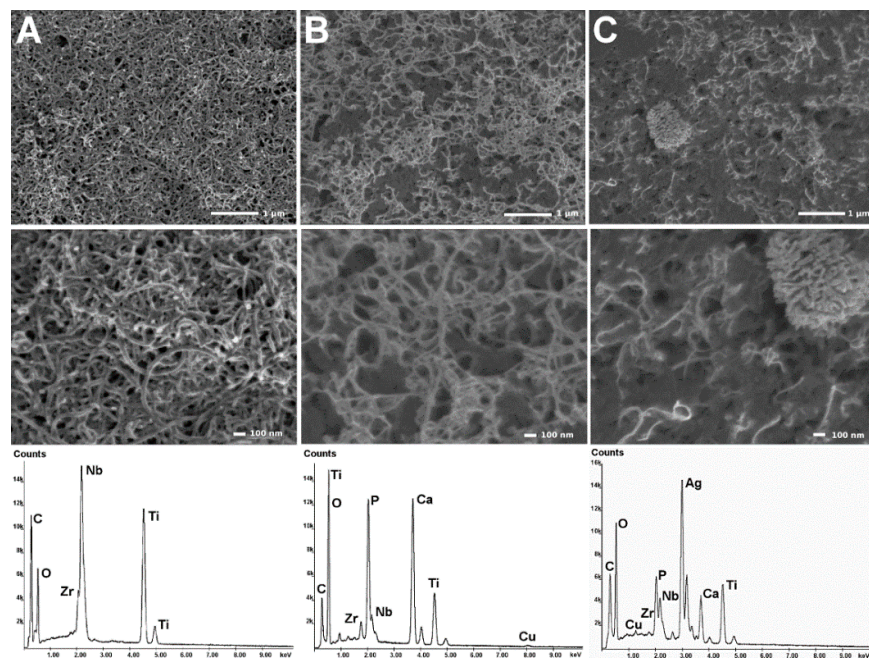
Figure 2. SEM surface topography with the energy dispersive spectrometer (EDS) spectrum of the sample: (**A**) 0.27CNT, (**B**) H0.27CNT, (**C**) m0.4CNT.

The SEM images (Figure 2) demonstrate a more uniform distribution of carbon nanotubes for the 0.27CNT sample than for the H0.27CNT sample. On the surface of the m0.4CNT sample, many agglomerates are present, as a result of the simultaneous deposition of nanosilver and nanocopper, which do not move into a bulk, but are absorbed on the HAp coating, resulting in decreased roughness (Table 3). The roughness values are similar to those previously reported [14].

Table 3. Surface roughness of the native material and deposited coatings.

Sample	Roughness S_a [μm]
MR	0.203
MRe	0.256
0.27CNT	0.098
H0.27CNT	0.980
M0.4CNT	0.618

3.2. Mechanical Studies

3.2.1. Nanoindentation

Figure 3 shows the load–displacement hysteresis curve as an example of the results of nanoindentation tests. Three stages of the nanoindentation test are observed: the raising load to a maximum value, the pause (to stabilize the probe at maximum depth), and offloading. An irregularity in the form of a step due to temperature drift, adjusted at the end of nanoindentation, can be observed.
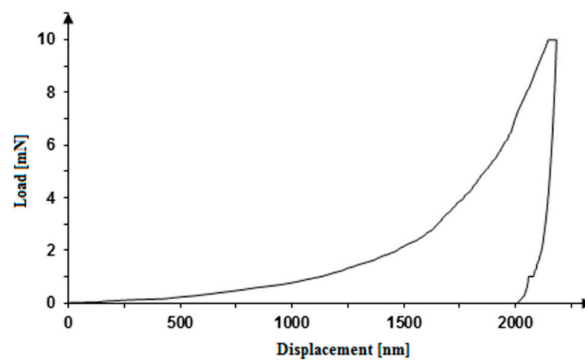
Figure 3. Nanoindentation load–displacement curve obtained for pure CNT coating (0.27CNT).

The exact values of measured mechanical properties are listed in Table 4. The lowest hardness values are demonstrated for H0.26CNT and m0.4CNT coatings due to the significant effect of etching on hardness. A 53-fold difference in the hardness is noticed between polished and etched specimens. The CNTs alone have the best hardness and wear resistance. The addition of softer nanoHAp decreases mechanical strength. The composite coating displays improved behavior, presumably because of a different coating architecture and the decisive role of metal nanoparticles. The hardness here measured is lower than the values previously reported in [44] as 0.37 to 0.58 GPa.

The elastic modulus values observed here are in line with some previous results for titanium, and much smaller for CNTs coating, so far reported as 60 MPa [14] and 113–130 MPa [16]. An increase in Young's modulus from 15 to 40 GPa [35] and from 12 to 19 GPa [44] was also observed. The reason for such discrepancies may be the high dependence of nanomechanical properties of the coating architecture, test parameters, and fractions of components.

Table 4. Mechanical properties and maximum indent depth for the substrate and achieved coatings.

| Sample	Nanohardness [GPa]	Reduced Young's Modulus [GPa]	Young's Modulus [GPa]	Maximum Indent Depth [nm]
I	3.758 ± 1.045	116.91 ± 16.32	83.32 ± 11.63	330.92 ± 36.61
MRe	0.071 ± 0.010	14.57 ± 2.21	9.44 ± 1.43	2358.11 ± 170.08
0.27CNT	0.101 ± 0.049	18.59 ± 5.66	14.17 ± 4.32	2069.67 ± 352.57
H0.27CNT	0.022 ± 0.015	7.46 ± 3.65	5.63 ± 2.76	4264.18 ± 1150.11
m0.4CNT	0.035 ± 0.019	11.72 ± 4.31	8.88 ± 3.26	3210.02 ± 817.53

Figures 4 and 5 show the 3D distribution of Young's modulus and nanohardness for the examined samples. Compared to the other materials, the native material after grinding (MR) reveals the biggest nanohardness and Young modulus.

The 3D Young's modulus (Figure 4) and nanohardness (Figure 5) distribution graphs show a highly non-uniform rough surface. The roughest is only a polished surface, lower roughness is observed for CNTs coating, and the etched surface and two other coatings show differences in Young's modulus in the range of 20 MPa. For hardness, the same effects can be noticed. The most heterogeneous are the H0.27CNT and m0.4CNT coatings, due either to appearing agglomerates or variable layer thickness, or both. The 0.27CNT specimen's nanohardness and Young's modulus distribution graphs show "uplifts," which could result from the probe's contact with the surface of the native material. Nevertheless, the 0.27CNT sample appears to possess a Young's modulus very similar to that of a human bone. Cuppone et al. reported that the cortical bone has an average Young's modulus value of 18.6 ± 1.9 GPa [47]. In conclusion, the results generally show that Young's modulus increases with rising nanohardness.
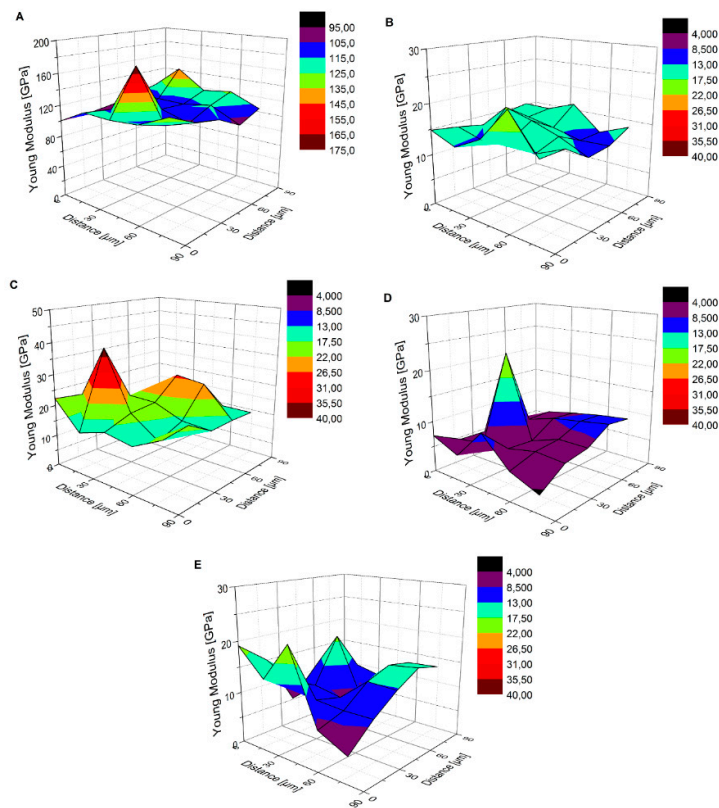
Figure 4. 3D Young's modulus distribution for: (**A**) native material after grinding (MR), (**B**) native material after etching (MRe), (**C**) CNTs coating (0.27CNT), (**D**) CNTs deposited on HAp coating (H0.27CNT), (**E**) mixed coating consisting of CNTs, nanoHAp, nanoAg and nanoCu (m0.4CNT).
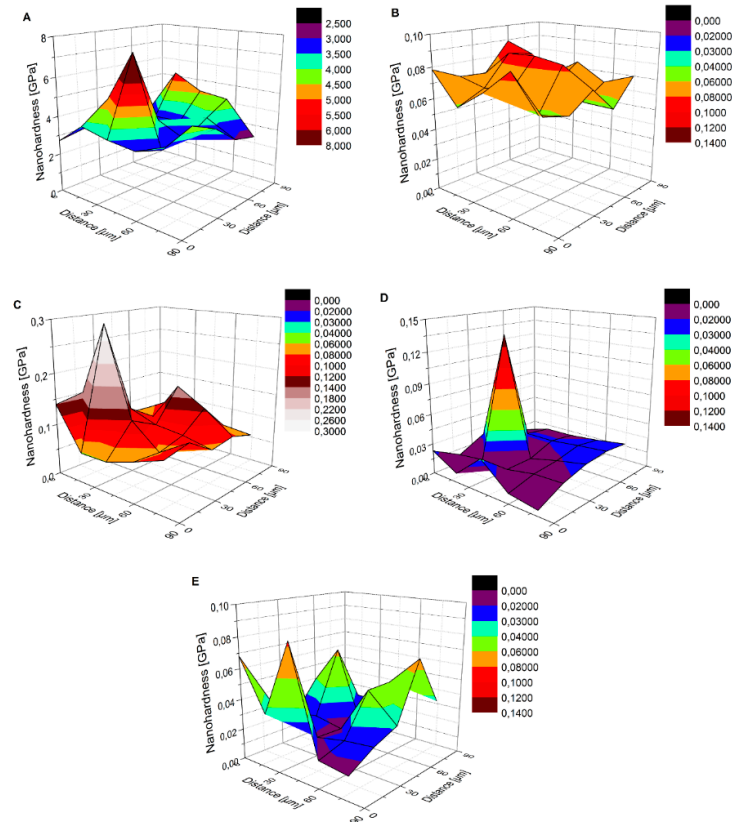
Figure 5. 3D nanohardness distribution for (**A**) native material after grinding (MR), (**B**) native material after etching (MRe), (**C**) CNTs coating (0.27CNT), (**D**) CNTs deposited on HAp coating (H0.27CNT), (**E**) mixed coating consisting of CNTs, nanHAp, nanoAg and nanoCu (m0.4CNT).

3.2.2. Nanoscratch Test

Figure 6 shows the relation of friction (F) on load (L) for each coating subjected to the nanoscratch test. The graphs describe a critical load (Lc) for every single measurement, represented by a vertical line indicating the moment of delamination for the carbon nanotube coating (0.27CNT), the carbon nanotube coating on hydroxyapatite (H0.27CNT) and the mixed coating consisting of carbon nanotubes, nanohydroxyapatite, nanosilver and nanocopper (m0.4CNT), respectively.

The values of the critical load (Lc) and critical friction (Fc), which indicate the load and friction under which the coating cracks or is delaminated, are shown in Table 5.

To conclude, the CNTs coating deposited on the Ti13Nb13Zr alloy (0.27CNT) has the best strength adhesion to the surface, while the worst adhesion is demonstrated by the composite coating (m0.4CNT). Application of HAp ceramics as an interlayer and its sintering does not improve the adhesion of the CNTs coating to the surface of titanium alloy. What is more, the addition of nanosilver and nanocopper to the composite coating further decreases adhesion, presumably due to the change in the particle size of nanometals caused by agglomeration in the bath. These results demonstrate that adhesion is best when the CNTs adhere directly to the surface, forming strong chemical bonds. Regretfully, these results cannot be compared to the adhesion strength 18–22 MPa measured by the Adhesion Test method [16] and 32 MPa measured by the F1044 shear bond strength test [35] as these methods are very different from the nanoscratch tests. On the other hand, during surgery and the period after implantation, the coatings are subject to shear stresses. Therefore, the nanoscratch method seems particularly suitable for determining real adhesion.
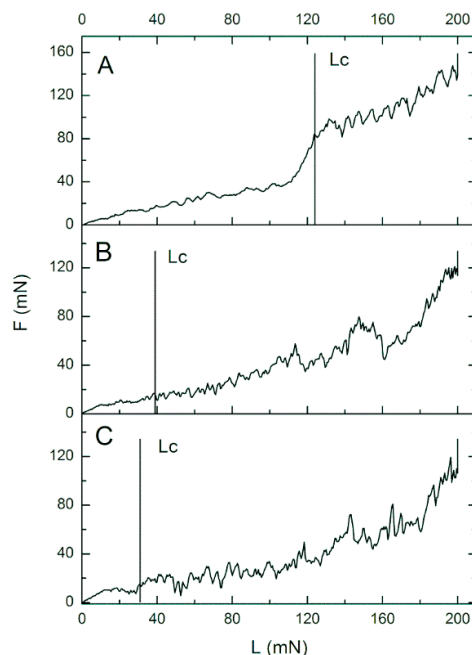
Figure 6. Friction (F) dependence on load (L) with the indicated critical load (Lc) for the single measurement of (**A**) the carbon nanotube coating on the surface of Ti13Nb13Zr (0.27CNT), (**B**) the carbon nanotube coating on the surface of the hydroxyapatite (H0.27CNT), (**C**) the mixed coating consisting of carbon nanotubes, nanohydroxyapatite, nanosilver and nanocopper (m0.4CNT).

Table 5. Parameters of coatings delamination.

Sample	Critical Friction (Fc) [mN]	Critical Load (Lc) [mN]
0.27CNT	89.42 ± 36.19	116.50 ± 32.07
H0.27CNT	39.96 ± 18.07	92.06 ± 34.3
m0.4CNT	29.56 ± 6.92	60.38 ± 10.21

3.3. Contact Angle Measurements

Figure 7 shows images of the water drops poured on the surface of all tested specimens. After etching, the surface of the Ti13Nb13Zr became hydrophobic, as the mean contact angle reached the value of 97.40°. This could be the result of the higher roughness of the etched surface (Table 3). The CNTs coating was found hydrophilic [48] with the angle value 56.50°, which means that the surface is proper for its application in implantology. Türka et al. achieved similar results for the contact angle of the CNTs after functionalization, 53.29° [49]. However, the CNTs–HAp and composite coatings are both hydrophobic, and as such they cannot be useful for implants. Prodana et al. explained the hydrophilicity of TiO_2/MWCNTs/HAp coating on titanium substrate by the appearance of C–O single bonds, and C=O and O–C=O more oxidized forms, which might be responsible for increasing surface hydrophilicity [20]. Nevertheless, during the electrophoretic deposition process, the pH rises at the cathodic substrate, resulting in deprotonation of carboxyl groups (COOH) and, thereby, functionalized CNTs become more negatively charged. Carboxyl groups (COO–) facilitate the electrostatic interaction of Ca^{2+} ions from HAp with CNTs [46]. Based on reports to date, and our research, the hydrophobic appearance of an arrangement of CNTs and porous HAp may be attributed to an occurrence of a specific architecture with a lesser ability to form van der Waals bonds between water and specimen surface. A similar explanation may be given regarding the composite materials, indicating the increased effects of nanohydroxyapatite, which may have a different microstructure to CNTs. Further attempts made with various forms of both components, oriented particularly towards better hydrophilicity, should give a more plausible solution.
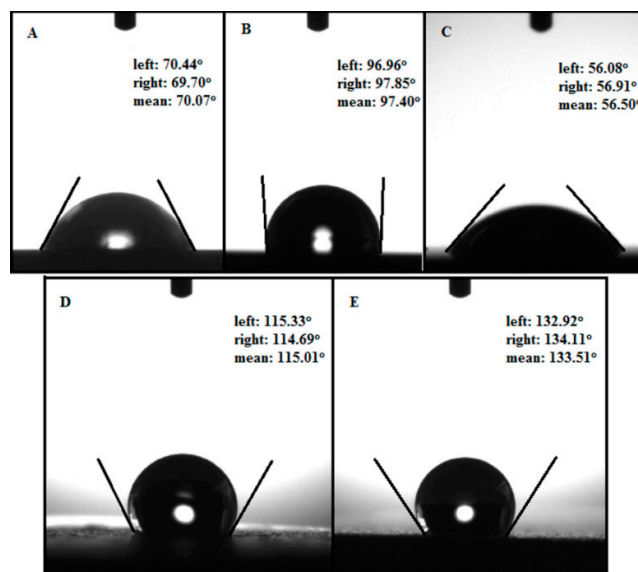
Figure 7. Contact angle (CA) for: (**A**) native material after grinding (MR), (**B**) native material after etching (MRe), (**C**) carbon nanotube coating on the surface of Ti13Nb13Zr (0.27CNT), (**D**) carbon nanotube coating on the surface of the hydroxyapatite (H0.27CNT), (**E**) the mixed coating consisting of carbon nanotubes, nanohydroxyapatite, nanosilver and nanocopper (m0.4CNT).

4. Conclusions

The multi-wall carbon nanotubes deposited on the surface of the Ti13Nb13Zr alloy by the electrophoretic method demonstrate a relatively high hardness and wear resistance, firm adhesion, and proper wettability, so they are suitable for surface treatment of the titanium implants made of the investigated alloy.

The hybrid coatings obtained by the formation of hydroxyapatite deposit, followed by a carbon nanotubes' layer, have lower adhesion strength, hardness, and less proper wettability, presumably due to the weak interface bonding between hydroxyapatite and carbon nanotubes, which is related to the properties of the ceramic material.

The composite layer has the lowest adhesion strength, hardness, and equally improper wettability, which can be attributed to weak bonding of components in the coating.

The obtained results provide evidence that the mutual bonding strength of all components and critical strength at the coating–substrate interface, are more significant determinants of mechanical properties than the components and the deposition process parameters.

Author Contributions: Conceptualization, B.M.-M.; Formal Analysis, M.B. and B.B.; Investigation, B.M.-M., D.R.-W. and M.B.; Methodology, B.M.-M., D.R.-W., M.B. and B.B.; Project administration, B.M.-M.; Resources, B.B.; Supervision, A.Z.; Visualization, D.R.-W.; Writing–Original Draft, B.M.-M. and D.R.-W.; Writing–Review and Editing, A.Z.

Conflicts of Interest: The authors declare no conflict of interest.

References

1. Ku, S.H.; Lee, M.; Park, C.B. Carbon-Based Nanomaterials for Tissue Engineering. *Adv. Healthc. Mater.* **2013**, *2*, 244–260.
2. Li, X.; Liu, X.; Huang, J.; Fan, Y.; Cui, F. Surface & Coatings Technology Biomedical investigation of CNT based coatings. *Surf. Coat. Technol.* **2011**, *206*, 759–766.

3. Dlugon, E.; Simka, W.; Fraczek-Szczypta, A.; Niemiec, W.; Markowski, J.; Szymanska, M.; Blazewicz, M. Carbon nanotube-based coatings on titanium. *Bull. Mater. Sci.* **2015**, *38*, 1339–1344.

4. Tanaka, M.; Sato, Y.; Zhang, M.; Haniu, H.; Okamoto, M.; Aoki, K.; Takizawa, T.; Yoshida, K.; Sobajima, A.; Kamanaka, T.; et al. In Vitro and In Vivo Evaluation of a Three-Dimensional Porous Multi-Walled Carbon Nanotube Scaffold for Bone Regeneration. *Nanomaterials* **2017**, *7*, 46.

5. Lahiri, D.; Ghosh, S.; Agarwal, A. Carbon nanotube reinforced hydroxyapatite composite for orthopedic application: A review. *Mater. Sci. Eng. C* 2012, *32*, 1727–1758.

6. Usui, Y.; Aoki, K.; Narita, N.; Murakami, N.; Nakamura, I.; Nakamura, K.; Ishigaki, N.; Yamazaki, H.; Horiuchi, H.; Kato, H.; et al. full papers Carbon Nanotubes with High Bone-Tissue Compatibility and Bone-Formation Acceleration Effects. **2008**, *8621*, 240–246.

7. Kalbacova, M.; Kalbac, M. Influence of single-walled carbon nanotube films on metabolic activity and adherence of human osteoblasts. **2007**, *45*, 2266–2272.

8. Lahiri, D.; Benaduce, A.P.; Rouzaud, F.; Solomon, J.; Keshri, A.K.; Kos, L.; Agarwal, A. Wear behavior and in vitro cytotoxicity of wear debris generated from hydroxyapatite – carbon nanotube composite coating. **2010**, *0494*, 1–12.

9. Matsuoka, M.; Akasaka, T.; Totsuka, Y.; Watari, F. Strong adhesion of Saos-2 cells to multi-walled carbon nanotubes. *Mater. Sci. Eng. B* **2010**, *173*, 182–186.

10. Akasaka, T.; Yokoyama, A.; Matsuoka, M.; Hashimoto, T.; Watari, F. Thin fi lms of single-walled carbon nanotubes promote human osteoblastic cells (Saos-2) proliferation in low serum concentrations. *Mater. Sci. Eng. C* **2010**, *30*, 391–399.

11. Hirschfeld, J.; Akinoglu, E.M.; Wirtz, D.C.; Hoerauf, A.; Bekeredjian-Ding, I.; Jepsen, S.; Haddouti, E.M.; Limmer, A.; Giersig, M. Long-term release of antibiotics by carbon nanotube-coated titanium alloy surfaces diminish biofilm formation by Staphylococcus epidermidis. *Nanomedicine Nanotechnology, Biol. Med.* **2017**, *13*, 1587–1593.

12. Bai, Y.; Prasad, M.; Song, I.; Ho, M.; Sung, T.; Watari, F.; Uo, M. Electrophoretic deposition of carbon nanotubes – hydroxyapatite nanocomposites on titanium substrate. *Mater. Sci. Eng. C* **2010**, *30*, 1043–1049.

13. Długoń, E.; Niemiec, W.; Frączek-Szczypta, A.; Jeleń, P.; Sitarz, M.; Błazewicz, M. Spectroscopic studies of electrophoretically deposited hybrid HAp/CNT coatings on titanium. *Spectrochim. Acta Part A Mol. Biomol. Spectrosc.* **2014**, *133*, 872–875.

14. Abrishamchian, A.; Hooshmand, T.; Mohammadi, M.; Najafi, F. Preparation and characterization of multi-walled carbon nanotube/hydroxyapatite nanocomposite film dip coated on Ti-6Al-4V by sol-gel method for biomedical applications: An in vitro study. *Mater. Sci. Eng. C* **2013**, *33*, 2002–2010.

15. Gopi, D.; Shinyjoy, E.; Kavitha, L. Influence of ionic substitution in improving the biological property of carbon nanotubes reinforced hydroxyapatite composite coating on titanium for orthopedic applications. *Ceram. Int.* **2015**, *41*, 5454–5463.

16. Gopi, D.; Shinyjoy, E.; Sekar, M.; Surendiran, M.; Kavitha, L.; Sampath Kumar, T.S. Development of carbon nanotubes reinforced hydroxyapatite composite coatings on titanium by electrodeposition method. *Corros. Sci.* **2013**, *73*, 321–330.

17. Pei, X.; Zeng, Y.; He, R.; Li, Z.; Tian, L.; Wang, J.; Wan, Q.; Li, X.; Bao, H. Single-walled carbon nanotubes/hydroxyapatite coatings on titanium obtained by electrochemical deposition. *Appl. Surf. Sci.* **2014**, *295*, 71–80.

18. Zhong, Z.; Qin, J.; Ma, J. Electrophoretic deposition of biomimetic zinc substituted hydroxyapatite coatings with chitosan and carbon nanotubes on titanium. *Ceram. Int.* **2015**, *41*, 8878–8884.

19. Zanello, L.P.; Zhao, B.; Hu, H.; Haddon, R.C. Bone cell proliferation on carbon nanotubes. *Nano Lett.* **2006**, *6*, 562–567.

20. Prodana, M.; Duta, M.; Ionita, D.; Bojin, D.; Stan, M.S.; Dinischiotu, A.; Demetrescu, I. A new complex ceramic coating with carbon nanotubes, hydroxyapatite and TiO 2 nanotubes on Ti surface for biomedical applications. *Ceram. Int.* **2015**, *41*, 6318–6325.

21. Chouirfa, H.; Bouloussa, H.; Migonney, V.; Falentin-Daudré, C. Review of titanium surface modification techniques and coatings for antibacterial applications. *Acta Biomater.* 2019, *83*, 37–54.

22. Sivaraj, D.; Vijayalakshmi, K. Substantial effect of magnesium incorporation on hydroxyapatite/carbon nanotubes coatings on metallic implant surfaces for better anticorrosive protection and antibacterial ability. *J. Anal. Appl. Pyrolysis* **2018**, *135*, 15–21.

23. Mukherjee, S.; Nandi, S.K.; Kundu, B.; Chanda, A.; Sen, S.; Das, P.K. Enhanced bone regeneration with carbon nanotube reinforced hydroxyapatite in animal model. *J. Mech. Behav. Biomed. Mater.* **2016**, *60*, 243–255.

24. Malik, M.A.; Wani, M.Y.; Hashim, M.A.; Nabi, F. Nanotoxicity: Dimensional and morphological concerns. *Adv. Phys. Chem.* **2011**, *2011*.

25. Teleanu, D.; Chircov, C.; Grumezescu, A.; Teleanu, R. Neurotoxicity of Nanomaterials: An Up-to-Date Overview. *Nanomaterials* **2019**, *9*, 96.

26. Mohanta, D.; Patnaik, S.; Sood, S.; Das, N. Carbon nanotubes: Evaluation of toxicity at biointerfaces. *J. Pharm. Anal.* **2019**.

27. Nawrotek, K.; Tylman, M.; Rudnicka, K.; Gatkowska, J.; Balcerzak, J. Tubular electrodeposition of chitosan-carbon nanotube implants enriched with calcium ions. *J. Mech. Behav. Biomed. Mater.* **2016**, *60*, 256–266.

28. Guan, K.; Zhang, L.; Zhu, F.; Sheng, H.; Li, H. Surface modification for carbon/carbon composites with Mg-CaP coating reinforced by SiC nanowire-carbon nanotube hybrid for biological application. *Appl. Surf. Sci.* **2019**, *489*, 856–866.

29. Khazeni, D.; Saremi, M.; Soltani, R. Development of HA-CNTs composite coating on AZ31 Magnesium alloy by cathodic electrodeposition. Part 2: Electrochemical and in-vitro behavior. *Ceram. Int.* **2019**, *45*, 11186–11194.

30. Alsagri, A.S.; Nasir, S.; Gul, T.; Islam, S.; Nisar, K.S.; Shah, Z.; Khan, I. MHD thin film flow and thermal analysis of blood with CNTs nanofluid. *Coatings* **2019**, *9(3),175*.

31. Przekora, A.; Benko, A.; Nocun, M.; Wyrwa, J.; Blazewicz, M.; Ginalska, G. Titanium coated with functionalized carbon nanotubes − A promising novel material for biomedical application as an implantable orthopaedic electronic device. *Mater. Sci. Eng. C* **2014**, *45*, 287–296.

32. Jacobs, C.B.; Peairs, M.J.; Venton, B.J. Analytica Chimica Acta Review: Carbon nanotube based electrochemical sensors for biomolecules. **2010**, *662*, 105–127.

33. Benko, A.; Nocuń, M.; Berent, K.; Gajewska, M.; Klita, Ł.; Wyrwa, J.; Błażewicz, M. Diluent changes the physicochemical and electrochemical properties of the electrophoretically-deposited layers of carbon nanotubes. *Appl. Surf. Sci.* **2017**, *403*, 206–217.

34. Sivaraj, D.; Vijayalakshmi, K. Novel synthesis of bioactive hydroxyapatite/f-multiwalled carbon nanotube composite coating on 316L SS implant for substantial corrosion resistance and antibacterial activity. *J. Alloys Compd.* **2019**, 1340–1346.

35. Maleki-Ghaleh, H.; Khalil-Allafi, J. Characterization, mechanical and in vitro biological behavior of hydroxyapatite-titanium-carbon nanotube composite coatings deposited on NiTi alloy by electrophoretic deposition. *Surf. Coatings Technol.* **2019**, *363*, 179–190.

36. Mohajernia, S.; Pour-Ali, S.; Hejazi, S.; Saremi, M.; Kiani-Rashid, A.R. Hydroxyapatite coating containing multi-walled carbon nanotubes on AZ31 magnesium: Mechanical-electrochemical degradation in a physiological environment. *Ceram. Int.* **2018**, *44*, 8297–8305.

37. Park, J.E.; Jang, Y.S.; Bae, T.S.; Lee, M.H. Multi-walled carbon nanotube coating on alkali treated TiO2 nanotubes surface for improvement of biocompatibility. *Coatings* **2018**, *8(5), 159*.

38. Fraczek-szczypta, A.; Jantas, D.; Ciepiela, F.; Grzonka, J.; Bernasik, A.; Marzec, M. Diamond & Related Materials Carbon nanomaterials coatings – Properties and in fl uence on nerve cells response. *Diam. Relat. Mater.* **2018**, *84*, 127–140.

39. Farrokhi-Rad, M.; Menon, M. Effect of Dispersants on the Electrophoretic Deposition of Hydroxyapatite-Carbon Nanotubes Nanocomposite Coatings. *J. Am. Ceram. Soc.* **2016**, *99*, 2947–2955.

40. Liu, S.; Li, H.; Su, Y.; Guo, Q.; Zhang, L. Preparation and properties of in-situ growth of carbon nanotubes reinforced hydroxyapatite coating for carbon/carbon composites. *Mater. Sci. Eng. C* **2017**, *70*, 805–811.

41. Boccaccini, B.C.T.Æ.A.R. Bioactive ceramic coatings containing carbon nanotubes on metallic substrates by electrophoretic deposition. **2006**, 8144–8151.

42. Constanda, S.; Stan, M.S.; Ciobanu, C.S.; Motelica-Heino, M.; Guégan, R.; Lafdi, K.; Dinischiotu, A.; Predoi, D. Carbon Nanotubes-Hydroxyapatite Nanocomposites for an Improved Osteoblast Cell Response. *J. Nanomater.* **2016**, *2016*.

43. Yi, C.; Bagchi, S.; Dmuchowski, C.M.; Gou, F.; Chen, X.; Park, C.; Chew, H.B.; Ke, C. Direct nanomechanical characterization of carbon nanotube - titanium interfaces. *Carbon N. Y.* **2018**, *132*, 548–555.

44. Sasani, N.; Vahdati Khaki, J.; Mojtaba Zebarjad, S. Characterization and nanomechanical properties of novel dental implant coatings containing copper decorated-carbon nanotubes. *J. Mech. Behav. Biomed. Mater.* **2014**, *37*, 125–132.

45. Zhao, X.; Chen, X.; Zhang, L.; Liu, Q.; Wang, Y.; Zhang, W.; Zheng, J. Preparation of Nano-Hydroxyapatite Coated Carbon Nanotube Reinforced Hydroxyapatite Composites. *Coatings* **2018**, *8*, 357.

46. Fathyunes, L.; Khalil-Allafi, J.; Moosavifar, M. Development of graphene oxide/calcium phosphate coating by pulse electrodeposition on anodized titanium: Biocorrosion and mechanical behavior. *J. Mech. Behav. Biomed. Mater.* **2019**, *90*, 575–586.

47. Cuppone, M.; Seedhom, B.B.; Berry, E.; Ostell, A.E. The Longitudinal Young's Modulus of Cortical Bone in the Midshaft of Human Femur and its Correlation with CT Scanning Data. *Calcif. Tissue Int.* **2004**, *74*, 302–309.

48. Sansotera, M.; Talaeemashhadi, S.; Gambarotti, C.; Pirola, C.; Longhi, M.; Ortenzi, M.A.; Navarrini, W.; Bianchi, C.L. Comparison of branched and linear perfluoropolyether chains functionalization on hydrophobic, morphological and conductive properties of multi-walled carbon nanotubes. *Nanomaterials* **2018**, *8*, 2–4.

49. Türk, S.; Altınsoy, I.; Çelebi Efe, G.; Ipek, M.; Özacar, M.; Bindal, C. 3D porous collagen/functionalized multiwalled carbon nanotube/chitosan/hydroxyapatite composite scaffolds for bone tissue engineering. *Mater. Sci. Eng. C* **2018**, *92*, 757–768.